



## Obrabotka metallov -

## Metal Working and Material Science

Journal homepage: [http://journals.nstu.ru/obrabotka\\_metallov](http://journals.nstu.ru/obrabotka_metallov)



### Determination of the main parameters of resistance spot welding of Al-5 Mg aluminum alloy

Viktor Kondratiev<sup>1, 2, a</sup>, Valeriy Gozbenko<sup>3, 4, b, \*</sup>, Roman Kononenko<sup>5, c</sup>,  
Marina Konstantinova<sup>5, d</sup>, Elena Guseva<sup>5, e</sup>

<sup>1</sup> A.P. Vinogradov Institute of Geochemistry of the Siberian Branch of the Russian Academy of Sciences, 1A Favorsky str., Irkutsk, 664033, Russian Federation





<sup>2</sup> Cherepovets State University, 5 Lunacharsky pr., Cherepovets, 162600, Russian Federation



<sup>3</sup> Irkutsk State Transport University, 15 Chernyshevskogo str., Irkutsk, 664074, Russian Federation

<sup>4</sup> Angarsk State Technical University, 60 Tchaikovsky str., Angarsk, 665835, Russian Federation

<sup>5</sup> Irkutsk National Research Technical University, 83 Lermontova str., Irkutsk, 664074, Russian Federation

<sup>a</sup>  <https://orcid.org/0000-0002-7437-2291>,  [imz@mail.ru](mailto:imz@mail.ru); <sup>b</sup>  <https://orcid.org/0000-0001-8394-0054>,  [vgozbenko@inbox.ru](mailto:vgozbenko@inbox.ru);

<sup>c</sup>  <https://orcid.org/0009-0001-5900-065X>,  [istu\\_politech@mail.ru](mailto:istu_politech@mail.ru); <sup>d</sup>  <https://orcid.org/0000-0002-8533-0214>,  [mavikonst@mail.ru](mailto:mavikonst@mail.ru);

<sup>e</sup>  <https://orcid.org/0000-0002-8719-7728>,  [el.guseva@rambler.ru](mailto:el.guseva@rambler.ru)

#### ARTICLE INFO

##### Article history:

Received: 06 March 2025

Revised: 07 April 2025

Accepted: 14 May 2025

Available online: 15 September 2025

##### Keywords:

Welding

Resistance Spot Welding (RSW)

Nugget

Heat-Affected Zone (HAZ)

Aluminum

Hardness

#### ABSTRACT

**Introduction.** The resistance spot welding (*RSW*) process has proven to be widely applicable across various industrial sectors, especially for mass production. Typical fields of application include aerospace, automotive, furniture manufacturing, and other industries. However, the *RSW* process presents certain challenges when welding aluminum and its alloys. Generally, aluminum alloys produce poor welds due to their physical and metallurgical properties such as oxide formation, thermal expansion and contraction, lower weldability, and the formation of intermetallic compounds. This study aims to evaluate the feasibility and mechanical characteristics of *RSW* joints in *Al-5 Mg* aluminum alloys. **The purpose** is to assess the potential of resistance spot welding for aluminum alloys and to determine the influence of key *RSW* parameters on the microstructure and properties of the weld. **Research methods.** *Al-5 Mg* aluminum alloy sheets in as-received condition were used. Spot welding was performed using a stationary resistance spot welding machine *MT-4240*. Samples for analysis were cut, polished, and subsequently examined under an optical microscope. Hardness measurements were carried out using a microhardness tester along two directions: radially across the nugget and through the sheet thickness, employing a 100 g load. An *Instron* electromechanical testing machine was utilized for shear testing at a constant traverse speed of 1 mm/min until complete joint failure at room temperature. The nugget diameter was measured on the fracture surface after shear tensile testing. **Results and Discussion.** Optimal input parameters for welding 2.5 mm thick aluminum sheets were identified, and three output variables were analyzed: tensile strength, joint hardness, and nugget diameter. It was observed that joint strength improved significantly with increased process parameters (welding current and welding period). Nugget diameter showed a clear correlation with input parameters related to current and welding period. An increase in process parameters, i.e., weld cycle time, electrode force, and welding current, led to an increase in nugget size. The ratio of weld strength to base metal strength reached approximately 0.9. It is demonstrated that resistance spot welding of 2.5 mm thick *Al-5 Mg* aluminum sheets is feasible and can be employed in various industrial applications.

**For citation:** Kondratiev V.V., Gozbenko V.E., Kononenko R.V., Konstantinova M.V., Guseva E.A. Determination of the main parameters of resistance spot welding of Al-5 Mg aluminum alloy. *Obrabotka metallov (tekhnologiya, oborudovanie, instrumenty) = Metal Working and Material Science*, 2025, vol. 27, no. 3, pp. 6–22. DOI: 10.17212/1994-6309-2025-27.3-6-22. (In Russian).

#### \* Corresponding author

Gozbenko Valeriy E., D.Sc. (Engineering), Professor

Irkutsk State Transport University,

15 Chernyshevskogo str.,

664074, Irkutsk, Russian Federation

Tel: +7 914 951-60-21, e-mail: [vgozbenko@inbox.ru](mailto:vgozbenko@inbox.ru)

## Introduction

Resistance spot welding (*RSW*) is widely used in the automotive, aerospace, construction, and energy industries for joining sheet metal components made of steel and aluminum alloys, as well as for creating dissimilar joints between steel and aluminum, aluminum and magnesium, and aluminum and titanium [1–10]. For example, the productivity of modern automated automotive assembly lines reaches up to 7 million spot welds per day [8, 9]. Aluminum alloys are extensively employed in the aerospace industry due to a combination of properties such as low density, high specific strength, good machinability, and corrosion resistance. Another significant advantage of aluminum alloys is their wide availability. The density of aluminum alloys is approximately one-third that of steel, which allows for a reduction in aircraft structural weight, improved fuel efficiency, and increased payload capacity.

For manufacturing critical load-bearing structural components of supersonic aircraft, where high strength is crucial, steel remains the preferred material [11–15]. However, aluminum alloys are widely used for wing panels, fuselage sections, empennage components, exhaust system parts, interior components, and engine turbine parts of modern aircraft. Aluminum alloys constitute between 50 % and 90 % of the mass of modern spacecraft. They have been extensively used in spacecraft such as *Soyuz*, *Progress*, space shuttles, satellites, and others [11–15]. Aluminum alloys are classified based on alloying systems such as *Al–Mg*, *Al–Mg–Li*, *Al–Cu–Li*, among others, which are the most common types applied in aerospace and automotive industries for high-strength engineering applications [14–18].

One of the key trends in the automotive industry is the reduction of vehicle weight. This goal is achieved by using materials with low specific weight, such as aluminum and its alloys, which in turn contributes to optimizing production costs [7–9]. Aluminum alloys are suitable metals for automotive applications because they can be easily cast and formed into required shapes and offer promising weight reduction compared to steel. The use of aluminum alloys in manufacturing body parts, cabin panels, wheel rims, and interior trim can reduce vehicle mass by more than 50 % [10, 11]. Owing to their combination of casting and deformation properties along with low specific weight, aluminum alloys stand out favorably compared to steels and are widely applied in the automotive sector.

For resistance spot welding of aluminum and its alloys, high-power welding guns are required due to the need for welding currents 2 to 3 times higher than those used for steel. This is caused by aluminum's higher electrical and thermal conductivity. Meanwhile, the welding period must be reduced to approximately one-third of that used for steel welding [1, 2].

Resistance spot welding (*RSW*) is a process of joining contacting metallic surfaces through heating generated by the electrical resistance to the current flowing through the parts being welded [1]. The welding process is controlled by three main parameters: *mechanical* (electrode force), *electrical* (welding current), and *temporal* (welding period). An electric current supplied to two overlapping sheets via coaxial electrodes is maintained for a sufficient duration to achieve localized fusion at the interface of the metal sheets. After the current is switched off, pressure is applied to form a strong joint along the fusion line. Subsequently, the molten metal cools down, forming a cast weld nugget within a confined volume.

The current density and applied pressure must be sufficient to form a solidified nugget but not so high as to expel molten metal from the weld zone. The welding current duration should be short enough to prevent excessive heating of the electrode surfaces. Electrode force, welding current magnitude, and welding period play a decisive role in the quality of the resistance spot weld. An electronic control unit is used in welding machines to monitor and regulate these welding parameters.

The quality and strength of welds produced by *RSW* are determined by the shape and size of the weld nuggets. Nugget size is a critical parameter that dictates the load-bearing capacity of the joint. There exists a direct correlation between heat generation and the size of the weld nugget during the *RSW* process. Heat generation, and consequently nugget size, is influenced by the following primary factors: contact resistance between the welded surfaces, welding current density, welding period, and thickness of the sheets being joined.

A key feature of *RSW* is the absence of the need for filler materials or fluxes. The competitive advantages of *RSW* over alternative metal joining methods, such as gas metal arc welding (*GMAW*), gas tungsten

arc welding (*GTAW*), and riveting, include the possibility for full process automation and integration into robotic production lines.

The main challenges limiting the application of *RSW* for aluminum alloys are:

1) *limited service life of contact electrodes*. The surface of aluminum alloys is characterized by the presence of an oxide film ( $Al_2O_3$ ) with high electrical resistance and non-uniform thickness [1, 2, 12–16]. When the sheets are compressed by the electrodes, the oxide film deforms unevenly, resulting in current concentration at localized contact points. The high current density in these areas causes intense heating, localized melting, and fusion between the copper electrode and aluminum, leading to erosive wear of the electrode's working surface [1, 2]. Changes in the geometry and composition of the electrode surface during operation cause instability in welding parameters and reduce weld strength [12–15].

2) *high welding current requirements*. To ensure the formation of high-quality welds in aluminum alloys by *RSW*, significantly higher welding currents are required compared to steels. This factor diminishes the potential energy efficiency advantages of aluminum alloys related to their lower density compared to steels [3, 4, 17, 18].

Existing studies on resistance spot welding (*RSW*) of aluminum alloys are predominantly focused on thick materials [19–21]. Thin-sheet aluminum alloys require separate consideration because differences in contact areas, thermal regimes, and electrical characteristics necessitate adjustments in welding parameters, including electrode force and current density [1, 2, 20–22]. Both alternating current (*AC*) and direct current (*DC*) power sources with varying frequencies are used for *RSW* [1, 2, 23–29], affecting energy transfer modes and optimal welding period for both stationary and portable equipment [1–3, 22, 28, 30, 31, 31–36]. Welding quality is also significantly influenced by external factors such as surface condition (roughness, contamination) [2–8], assembly accuracy [9], electrode condition (wear) [9–14], and the precision of positioning the welded parts (axial and angular misalignment) [20–22].

Aluminum alloys are highly sensitive to oxidation under environmental exposure. The oxide film formed on the surface ( $Al_2O_3$ ) exhibits high electrical resistance, which leads to increased heat generation at the contact zone during welding. Insufficient surface preparation aimed at oxide film removal can cause aluminum adhesion to the electrode material, accelerated electrode degradation, and poor-quality welds [1–5, 36–38]. Some studies have investigated the surface characteristics of aluminum alloy welds produced by *RSW* [3–8]; however, only a few reports document a significant decrease in hardness within the weld zone [1–4] for various aluminum alloy grades. Several works address the reduction in weld joint strength relative to the base metal and analyze the fracture behavior in the central weld nugget zone [29, 39].

This study aims to investigate the influence of resistance spot welding (*RSW*) parameters on the microstructure and mechanical properties of weld joints made from *Al-5 Mg* aluminum alloy.

**The objectives of this work** are:

- 1) to evaluate the applicability of resistance spot welding (*RSW*) for joining *Al-5 Mg* aluminum alloy;
- 2) to determine the effect of key *RSW* parameters on the microstructure and mechanical properties of the weld joint.

## Materials and experimental procedure

The *RSW* process cycle diagram and the lap joint configuration used for tensile shear testing are shown in Figs. 1 and 2, respectively.

For welding, 2.5 mm thick sheets of *Al-5 Mg* aluminum alloy (*GOST 21631-2023*) were used. Surface preparation of the sheets included the following steps: preliminary degreasing, followed by etching in a 4 % sodium hydroxide (*NaOH*) solution for 10 minutes, and subsequent treatment in a 2 % nitric acid (*HNO<sub>3</sub>*) solution for 5 minutes to remove the oxide film. Welding was performed on a stationary resistance spot welding machine *MTN-100.01*. The *RSW* process scheme and cycle diagram are presented in Fig. 2.

Shear tensile tests were conducted on a universal electromechanical testing machine *Instron* at room temperature, with a constant traverse speed of 1 mm/min until complete joint failure. The weld nugget diameter was measured on the fracture surface after the shear tensile test. Load values at shear and nugget diameter were calculated as the arithmetic mean of five measurements for each test series.

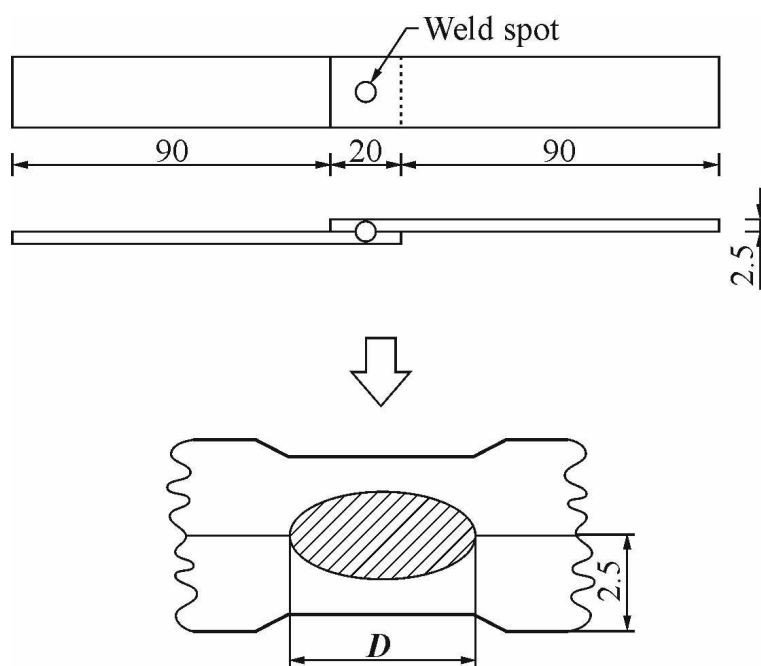


Fig. 1. Dimensions of the lap joint specimen produced by resistance spot welding (RSW) for tensile testing

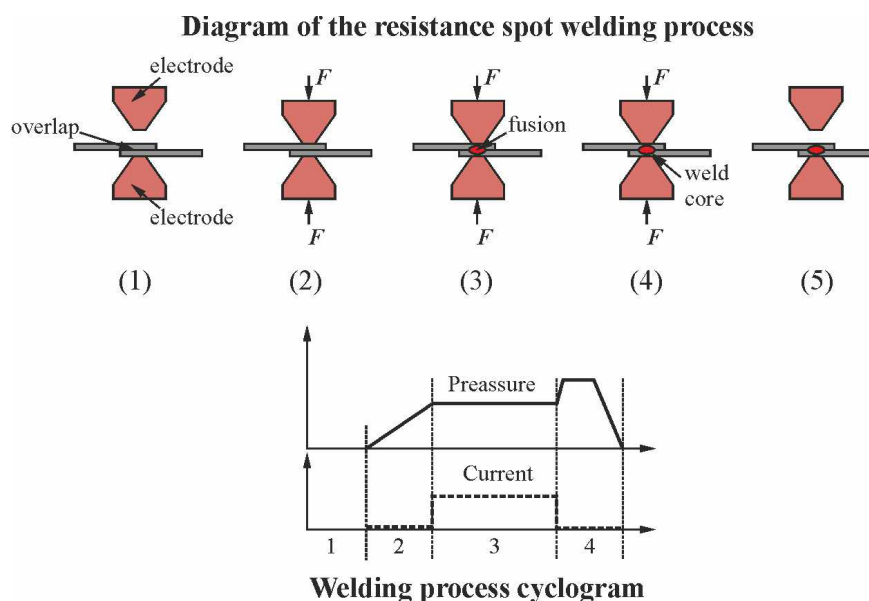


Fig. 2. Process scheme and cycle diagram of resistance spot welding (RSW)

For resistance spot welding (RSW) of 2.5 mm thick aluminum alloys, three variable parameters were used: welding current (ranging from 5 to 30 kA), welding period (from 1 to 5 seconds), and electrode force (from 2,000 to 5,000 N). The experiment consisted of thirteen series, each including welding of five samples: four for static shear tensile testing and one for metallographic analysis and hardness measurement.

Samples for metallographic analysis and hardness testing were cut perpendicular to the longitudinal direction of the welded specimens from the central region of the joint. Preparation of metallographic specimens involved cutting samples into 12 × 12 mm blanks, grinding, polishing, and etching to reveal the microstructure. Microstructure examination was performed using an optical microscope *Mikromed 2*. Hardness measurements were carried out in two directions (along the nugget radius and through the sheet thickness) using a microhardness tester with a 100 g load.



## Results and Discussion

The welds produced by resistance spot welding (*RSW*) demonstrated satisfactory surface quality across the entire range of tested parameters. Changes in the diameter and depth of electrode indentation were observed depending on the welding mode. Metallographic analysis revealed no internal defects such as porosity or shrinkage cavities within the cast structure of the weld nugget.

Fig. 3 shows the general microstructure of the weld joint, illustrating characteristic structural zones including the fusion zone and the heat-affected zone (*HAZ*). In the cast structure region (Fig. 3, *a*, *b*), a fine-grained recrystallized microstructure with equiaxed grains is observed, along with insoluble  $FeAl_3$  intermetallic inclusions (black) and a narrow zone of columnar crystals oriented along the heat dissipation direction during solidification. The heat-affected zone (*HAZ*), adjacent to the fusion zone (Fig. 3, *c*), is characterized by a dendritic structure. The base metal microstructure (Fig. 3, *d*) consists of grains elongated in the rolling direction.

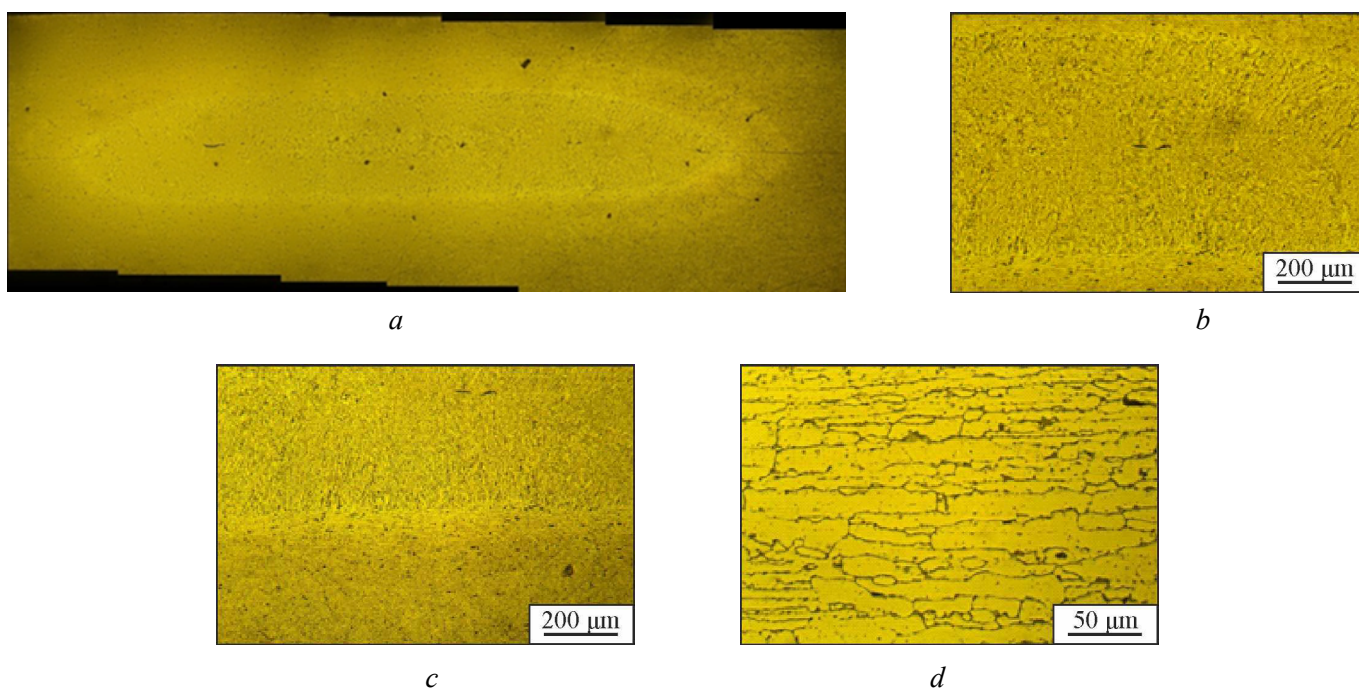


Fig. 3. Microstructure of a welded joint obtained by resistance spot welding (*RSW*):

*a* – general view of the welded joint; *b* – microstructure of the cast zone of the weld core; *c*) transition zone from the weld core to the heat-affected zone (*HAZ*); *d* – microstructure of the base material

To study the effect of welding period on the weld microstructure, metallographic analyses were performed on samples welded at various welding periods (from 33.4 ms to 167.0 ms) at a fixed welding current of 12 kA. It was found that increasing the welding period in this range leads to growth in grain size of equiaxed, dendritic, and columnar structures within the fusion zone. No significant changes in grain size or microstructure were detected in the *HAZ* compared to the base metal. However, welding periods exceeding 167.0 ms caused grain growth in the *HAZ* adjacent to the fusion zone relative to the base material, attributed to increased heat input during welding.

In the fusion zones of welds produced at the minimum welding current, a columnar grain structure with a pronounced liquation zone at the fusion boundary was observed (Fig. 3, *b*). The extent of the liquation zone increased at lower welding currents. Increasing the welding current resulted in a significant enlargement of the columnar grains in the fusion zone. Additionally, equiaxed grain regions formed in the central part of the fusion zone, indicating decreased cooling rates and thermal gradients. Grain coarsening was also noted in the *HAZ* of welds produced at higher welding currents.

Raising the welding current to 17 kA led to the formation of finer equiaxed grains in the fusion zone. The increase in welding current from 12 kA to 17 kA caused deeper electrode indentation into the sheets, reducing the distance between the cooled electrode and the center of the fusion zone. Consequently, the thermal gradient ( $G$ ) in the fusion zone increased. The diameter of the fusion zone was largely determined by welding current and welding period. A higher thermal gradient in the weld metal promotes the formation of a fine-grained microstructure during solidification, which is consistent with findings reported in references [1–7].

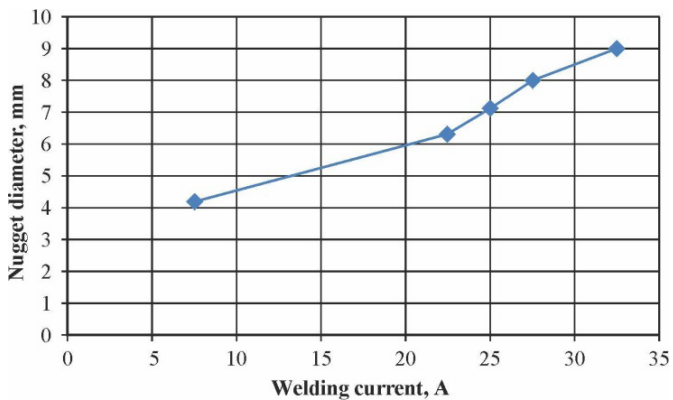


Fig. 4. Dependence of the nugget diameter on the welding current (RSW)

The dependence of the fusion zone diameter on welding current and welding period is presented in Figs. 4 and 5. A monotonic increase in the fusion zone diameter is observed with increasing welding current up to the maximum value achievable by the equipment used (Fig. 4). This trend is attributed to the increased heat input with rising welding current and is consistent with findings reported for carbon steels [1]. The results indicate that the applied electrode force was insufficient to cause the expulsion effect and the subsequent reduction in fusion zone diameter, since despite a small amount of expulsion occurring at 28.7 kA, no decrease in fusion zone diameter was observed (Fig. 4).

Several researchers have noted the possibility of increasing welding current without metal expulsion by increasing electrode force [2–5]. Metallographic analysis of samples welded at high current values revealed incomplete metal expulsion. Furthermore, welding current affects the depth of electrode indentation on the metal surface. All welds exhibited electrode indentations, the depth of which was largely determined by the welding current magnitude.

Electrode force has a minor effect on the fusion zone diameter for values up to 4,000 N. However, when the force exceeds this value, a slight decrease in fusion zone diameter is observed (Fig. 6). This effect can be explained by improved contact between the welded surfaces, resulting in reduced electrical resistance and heat input at higher electrode forces. The influence of the contact interface between the sheets on changes in fusion zone size depending on electrode compression force is also reported in studies [19–22].

The effect of electrode force on indentation depth was negligible within the investigated range. For detailed analysis of the electrode force effect on thickness reduction of the welded sheets, measurements were conducted at an intermediate welding current of 26.4 kA and welding period of cycle over a load range from 2,354 to 4,709 N. It was found that electrode force does not significantly affect indentation depth, while all welds showed an approximate 10% reduction in sheet thickness.

To evaluate the strength and load-bearing capacity of the welds, tensile tests were performed (Table 1).

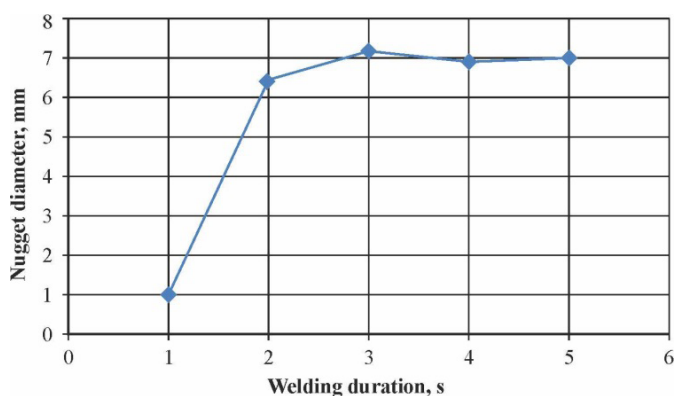


Fig. 5. Effect of welding period on the nugget size

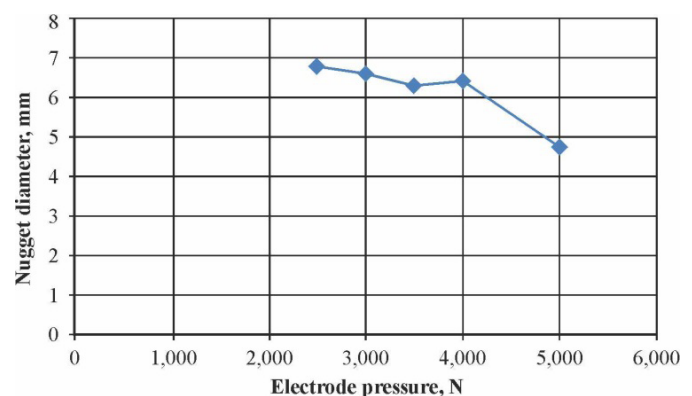


Fig. 6. Effect of the electrode force on the nugget

Table 1

Values of ultimate strength, nugget diameter, and average microhardness

Exp. No.	Tensile strength, MPa	Nugget diameter, mm	Average microhardness, HV
Base metal	272	—	94
1	231	7.91	110
2	220	7.68	105
3	228	7.62	103
4	218	7.59	98
5	198	6.94	103
6	187	6.85	101
7	210	7.20	106
8	203	6.87	101
9	189	7.12	106

Table 1 also presents results reflecting the influence of welding parameters on joint strength, fusion zone diameter, and hardness. It was found that increasing electrode force from 2 kN to 3 kN and welding current from 7 kA to 8 kA leads to a significant increase in tensile strength. Changes in welding period from 15 ms to 25 ms had little effect on joint strength.

To characterize the mechanical properties of the weld joint, *Vickers* microhardness was measured in the weld zone (Fig. 7). It was found that microhardness in the fusion zone increases with rising welding current and welding period. Maximum hardness values reached 110 HV and 107 HV. Average hardness values in the fusion zone exceeded that of the base metal (Fig. 7, red line), indicating a reduction in weld ductility compared to the base material.

Resistance spot welding (*RSW*) is a thermo-mechanical joining process in which heat plays a central role in forming a bond between the welded components. According to the *Joule-Lenz* law, the amount of heat generated during *RSW* is determined by the welding current, welding period, and the electrical resistance of the materials involved. Therefore, welding current, welding period, and electrode force are the primary parameters governing the welding process and, consequently, the quality of the weld joint (see Fig. 2). The *RSW* process cycle diagram typically reflects the variation of these three parameters over time and helps identify optimal ranges to achieve the desired weld characteristics [1–7].

It is well known that insufficient welding current can result in cold welding, whereas excessive welding current may cause metal expulsion from the fusion zone, as well as the formation of internal porosity or cracks within the cast microstructure. Insufficient electrode force may lead to molten metal spreading along the fusion boundary, while excessive force can reduce heat generation efficiency due to lowered contact resistance [1].

During welding, as the metal temperature rises, its electrical resistance also increases. The total resistance in the welding circuit (including the resistance of the welding machine, electrodes, and welded parts) determines the welding current magnitude. To form a molten zone in *RSW*, a certain value of total electrical resistance in the circuit must be ensured, which is the sum of resistances at each current path section through the welded workpieces [1, 2]. Higher total resistance improves weldability [1]. The total resistance depends

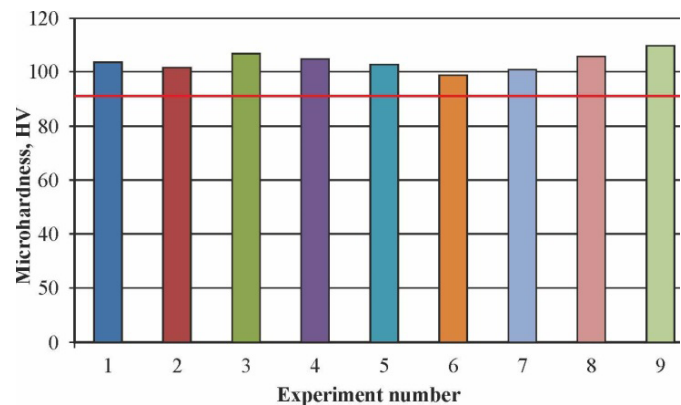


Fig. 7. Values of microhardness of the weld versus experiment number

on the surface condition of the welded materials and electrodes, electrode surface geometry, and electrode force. Maximum heat generation occurs at the contact interface between the welded parts, where the main electrical resistance is concentrated. Meanwhile, the high thermal conductivity of copper electrodes and their intensive water cooling prevent the base metal surface from reaching melting temperature.

As the temperature rises in the zone of maximum electrical resistance, metal melting and molten zone (weld nugget) formation occur. Simultaneously, the welded sheets thin, and the distance between electrodes decreases under electrode force, reducing the overall dynamic resistance. If the molten metal volume becomes too large for the surrounding solid metal to contain under the applied force, molten metal expulsion from the weld zone occurs. Increasing electrode force reduces electrical resistance by improving the contact between sheets and smoothing surface irregularities.

The efficiency of energy absorption and the growth rate of the fusion zone depend on the geometrical dimensions of the welded parts [10–15]. However, classical *RSW* studies [1, 2] often overlooked this factor, and most *RSW* control systems are optimized for welding parts of identical dimensions. Many researchers [1–12] aim to optimize *RSW* parameters to achieve a stable process and produce welds with specified properties. The significant influence of welding current and welding period on the quality of spot welds is consistently emphasized.

Authors [1–5] identify welding current, welding period, and electrode force as the main parameters of the resistance spot welding (*RSW*) process. To achieve an optimal fusion nugget diameter, increased values of welding current and welding period are recommended [1–3]. At the same time, other studies demonstrate a direct correlation of the fusion zone diameter with welding current and welding period, and an inverse correlation with electrode force [5–8].

The morphology of *RSW* joints in metal-to-metal connections is characterized by three distinct zones: the fusion zone (*FZ*), the heat-affected zone (*HAZ*), and the base metal (*BM*) (Fig. 3). The fusion zone represents the cast nugget formed due to melting and subsequent solidification of the welded metals. The heat-affected zone is the region that does not melt but undergoes microstructural changes due to heat transfer from the fusion zone. Microstructural analysis of samples obtained in this work also revealed these three characteristic zones (Fig. 3), with significant differences in microstructure within each zone. Both *FZ* and *HAZ* exhibit columnar dendrites oriented in a specific direction. Porosity formation in the cast structure is typically associated with surface contamination and possible hydrogen saturation of the metal. The absence of porosity in the fusion zone in this study indicates sufficient heat input to ensure quality melting of the base metal and formation of a strong joint.

Comparison of the microstructure between the *HAZ* and *FZ* shows larger columnar dendrite grains forming at the fusion boundary. The formation of columnar dendrites in both zones is driven by a high solidification rate ( $R$ ) and a steep thermal gradient ( $G$ ) between the molten metal (approximately 600 °C) and the base metal (at room temperature). Under these conditions, the undercooling criterion required for planar solidification at the solid-liquid interface is not met [1–7], meaning the  $G/R$  ratio is insufficient to suppress dendritic growth. The smaller size of columnar dendrites in the fusion zone is related to a higher cooling rate (i.e., faster solidification), attributed to the high thermal conductivity of aluminum alloys (120–180 W/m·K) [1, 5, 9, 12–15].

The cooling rate decreases from the fusion zone through the *HAZ* to the base metal, which acts as a heat sink. This is because thermal conductivity is the primary factor controlling cooling rate. Consequently, the  $G \times R$  value in the *HAZ* is lower compared to the fusion zone, resulting in coarser grains.

The size and shape of the fusion zone are key criteria for assessing *RSW* joint quality (Fig. 3, *a*) [1, 2, 5, 16–19]. In this study, the fusion zone diameter ( $D_{FZ}$ ) ranged from 1.33 to 7.61 mm. Each value represents an average of at least three measurements. A fusion zone diameter exceeding 7 mm is considered critical by several authors [1, 2] regarding its influence on the joint's mechanical strength. The increase in fusion zone size is attributed to the high heat input under the applied welding conditions.

Shear tensile strength is another important criterion used to evaluate the quality of resistance spot welded joints. In the conducted experiments, the shear tensile strength of nine welded samples ranged from 179 to 231 MPa (Table 1). The maximum shear tensile strength was achieved at a fusion zone diameter of 7.91 mm.



In conclusion, the *RSW* process is characterized by a complex interaction of multiple factors. However, the primary controllable parameters are welding current, electrode force, and welding period, all of which significantly affect the quality of the welded joint. Table 2 presents a summary of the influence of these parameters on the *RSW* process and weld quality, along with corresponding optimization measures based on a review of the literature [1–23].

Table 2

### Recommendations for optimizing the basic parameters of contact spot welding

Process variables	Effect on the welding point	Optimization measures
Welding current	Size and shape of the weld; Occurrence of expulsion; Shear and tensile strength form the microstructure of the weld	It is necessary to use a process modeling and experimentation to find the optimal combination for a specific process
Weld period	Tensile strength, peeling, and shear strength of welded joints	It is necessary to apply variation rather than a constant value during the process
Electrode force	Energy efficiency of the process; Occurrence of molten metal expulsion; Specific features of weld core solidification during spot welding	It is necessary to apply variation rather than a constant value during the process

In conclusion, it should be noted that achieving high-quality welds of aluminum alloys by resistance spot welding (*RSW*) requires careful selection of an optimal combination of welding cycle parameters. Specifically, to attain high shear tensile strength and welds with a large fusion zone diameter, it is essential to consider the potential occurrence of undesirable phenomena such as metal expulsion, spatter, cold welding, or formation of an insufficiently sized fusion zone. A review of the literature [1–23] indicates that welding current is the key parameter determining heat input during welding and is also the most easily adjustable parameter. Additionally, the application of variable electrode force, implemented via an electric servomechanism, can improve process stability and enhance weld quality [14–23].

Future research will focus on optimizing resistance spot welding parameters for aluminum alloys of various thicknesses.

## Conclusions

1. In resistance spot welding (*RSW*) of *Al-5 Mg* aluminum alloy, an increase in welding current and welding period leads to higher heat input and, consequently, an increase in the fusion zone diameter. The shear tensile strength of the welded joint also increases with rising welding current and welding period, which is attributed to the enlargement of the fusion zone diameter — a key factor determining joint strength.

2. For resistance spot welding (*RSW*) of 2.5 mm thick lap joints of *Al-5 Mg* aluminum alloy, the optimal parameters ensuring a shear tensile strength of 238 MPa are: electrode force of 3,000 N, welding current of 12 kA, and welding period of 25 ms.

## References

1. Kochergin K.A. *Kontaknaya svarka* [Contact welding]. Leningrad, Mashinostroenie Publ., 1987. 240 p.
2. Orlov B.D. *Tekhnologiya i oborudovanie kontaktnoi svarki* [Technology and equipment of contact welding]. Moscow, Mashinostroenie Publ., 1986. 352 p.
3. Zhou K., Yao P. Overview of recent advances of process analysis and quality control in resistance spot welding. *Mechanical Systems and Signal Processing*, 2019, vol. 124, pp. 170–198, DOI: 10.1016/j.ymssp.2019.01.041.
4. Hao M., Osman K.A., Boomer D.R., Newton C.J. Developments in characterization of resistance spot welding of aluminum. *Welding Journal – Including Welding Research Supplement*, 1996, vol. 75 (1), pp. 1–4. Available at:

<https://www.scopus.com/record/display.uri?eid=2-s2.0-0029777851&origin=inward&txGid=43eb57982320fc23bd6ff9a0a6c0a142> (accessed 07.08.2025).

5. Manladan S.M., Yusof F., Ramesh S., Fadzil M., Luo Z., Ao S. A review on resistance spot welding of aluminum alloys. *The International Journal of Advanced Manufacturing Technology*, 2017, vol. 90, pp. 605–634. DOI: 10.1007/s00170-016-9225-9.

6. Zhang Y., Li Y., Luo Z., Yuan T., Bi J., Wang Z.M., Wang Z.P., Chao Y.J. Feasibility study of dissimilar joining of aluminum alloy 5052 to pure copper via thermo-compensated resistance spot welding. *Materials & Design*, 2016, vol. 106, pp. 235–246. DOI: 10.1016/j.matdes.2016.05.117.

7. Zhang W., Xu J. Advanced lightweight materials for automobiles: A review. *Materials & Design*, 2022, vol. 221, p. 110994. DOI: 10.1016/j.matdes.2022.110994.

8. Sateesh N., Subbiah R., Nookaraju B.Ch, Nagaraju D. Siva. Achieving safety and weight reduction in automobiles with the application of composite material. *Materials Today: Proceedings*, 2022, vol. 62, pp. 4469–4472. DOI: 10.1016/j.matpr.2022.04.936.

9. Taub A., Moor E. De, Luo A., Matlock D.K., Speer J.G., Vaidya U. Materials for automotive lightweighting. *Annual Review of Materials Research*, 2019, vol. 49 (1), pp. 327–359. DOI: 10.1146/annurev-matsci-070218-010134.

10. Zhang Y., Shan H., Li Y., Guo J., Luo Z., Ma C. Yong. Joining aluminum alloy 5052 sheets via novel hybrid resistance spot clinching process. *Materials & Design*, 2017, vol. 118, pp. 36–43. DOI: 10.1016/j.matdes.2017.01.017.

11. Ambroziak A., Korzeniowski M. Using resistance spot welding for joining aluminium elements in automotive industry. *Archives of Civil and Mechanical Engineering*, 2010, vol. 10 (1), pp. 5–13. DOI: 10.1016/S1644-9665(12)60126-5.

12. Qiu R., Zhang Z., Zhang K., Shi H., Ding G. Influence of welding parameters on the tensile shear strength of aluminum alloy joint welded by resistance spot welding. *Journal of Materials Engineering and Performance*, 2011, vol. 20, pp. 355–358. DOI: 10.1007/s11665-010-9703-4.

13. Li Z., Hao C., Zhang J., Zhang H. Effects of sheet surface conditions on electrode life in resistance welding aluminum. *Welding Journal*, 2007, vol. 86 (4).

14. Qiu R., Li J., Shi H., Yu H. Characterization of resistance spot welded joints between aluminum alloy and mild steel with composite electrodes. *Journal of Materials Research and Technology*, 2023, vol. 24, pp. 1190–1202. DOI: 10.1016/j.jmrt.2023.03.069.

15. Pan B., Sun H., Shang S.-L., Wen W., Banu M., Simmer J.C., Carlson B.E., Chen N., Liu Z.-K., Zheng Z., Wang P., Li J. Corrosion behavior in aluminum/galvanized steel resistance spot welds and self-piercing riveting joints in salt spray environment. *Journal of Manufacturing Processes*, 2021, vol. 70, pp. 608–620. DOI: 10.1016/j.jmapro.2021.08.052.

16. Baek S., Go G.Y., Park J.-W., Song J., Lee H.-c., Lee S.-J., Lee S., Chen C., Kim M.-S., Kim D. Microstructural and interface geometrical influence on the mechanical fatigue property of aluminum/high-strength steel lap joints using resistance element welding for lightweight vehicles: experimental and computational investigation. *Journal of Materials Research and Technology*, 2022, vol. 17, pp. 658–678. DOI: 10.1016/j.jmrt.2022.01.041.

17. Arumugam A., Pramanik A. A review on the recent trends in forming composite joints using spot welding variants. *Journal of Composites Science*, 2024, vol. 8 (4), p. 155. DOI: 10.3390/jcs8040155.

18. Aslanlar S., Ogur A., Ozsarac U., Ilhan E. Welding time effect on mechanical properties of automotive sheets in electrical resistance spot welding. *Materials & Design*, 2008, vol. 29 (7), pp. 1427–1431. DOI: 10.1016/j.matdes.2007.09.004.

19. Matsushita M., Ikeda R., Oi K. Development of a new program control setting of welding current and electrode force for single-side resistance spot welding. *Welding in the World*, 2015, vol. 59, pp. 533–543. DOI: 10.1007/s40194-015-0228-1.

20. Chang B.H., Zhou Y. Numerical study on the effect of electrode force in small-scale resistance spot welding. *Journal of Materials Processing Technology*, 2003, vol. 139 (1–3), pp. 635–641. DOI: 10.1016/S0924-0136(03)00613-7.

21. Podrżaj P., Jerman B., Simončič S. Poor fit-up condition in resistance spot welding. *Journal of Materials Processing Technology*, 2016, vol. 230, pp. 21–25. DOI: 10.1016/j.jmatprotec.2015.11.009.

22. Yu J. New methods of resistance spot welding using reference waveforms of welding power. *International Journal of Precision Engineering and Manufacturing*, 2016, vol. 17, pp. 1313–1321. DOI: 10.1007/s12541-016-0156-z.



23. Zhang W., Sun D., Han L., Liu D. Interfacial microstructure and mechanical property of resistance spot welded joint of high strength steel and aluminium alloy with 4047 AlSi12 interlayer. *Materials & Design*, 2014, vol. 57, pp. 186–194. DOI: 10.1016/j.matdes.2013.12.045.

24. Pouranvari M., Marashi S.P.H. Critical review of automotive steels spot welding: process, structure and properties. *Science and Technology of Welding and Joining*, 2013, vol. 18 (5), pp. 361–403. DOI: 10.1179/1362171813Y.0000000120.

25. Karlina A.I., Kondrat'ev V.V., Kolosov A.D., Balanovskiy A.E., Ivanov N.A. Production of new nanostructures for modification of steels and cast irons. *IOP Conference Series: Materials Science and Engineering*, 2019, vol. 560 (1), p. 012183. DOI: 10.1088/1757-899X/560/1/012183.

26. Balanovsky A.E., Shtayger M.G., Kondrat'ev V.V., Van Huy V., Karlina A.I. Plasma-arc surface modification of metals in a liquid medium. *IOP Conference Series: Materials Science and Engineering*, 2018, vol. 411 (1), p. 012013. DOI: 10.1088/1757-899X/411/1/012013.

27. Konstantinova M.V., Balanovskiy A.E., Gozbenko V.E., Kargapoltsev S.K., Karlina A.I., Shtayger M.G., Guseva E.A., Kuznetsov B.O. Application of plasma surface quenching to reduce rail side wear. *IOP Conference Series: Materials Science and Engineering*, 2019, vol. 560 (1), p. 012146. DOI: 10.1088/1757-899X/560/1/012146.

28. Ivanchik N.N., Balanovsky A.E., Shtayger M.G., Sysoev I.A., Karlina A.I. Capability enhancement of production of activating fluxes for arc welding using ultradispersed products of silicon waste processing. *IOP Conference Series: Materials Science and Engineering*, 2018, vol. 411 (1), p. 012035. DOI: 10.1088/1757-899X/411/1/012035.

29. Yelemessov K., Baskanbayeva D., Martyushev N.V., Skeebe V.Y., Gozbenko V.E., Karlina A.I. Change in the properties of rail steels during operation and reutilization of rails. *Metals*, 2023, vol. 13, p. 1043. DOI: 10.3390/met13061043.

30. Balanovsky A.E., Shtayger M.G., Grechneva M.V., Kondrat'ev V.V., Karlina A.I. Comparative metallographic analysis of the structure of St3 steel after being exposed to different ways of work-hardening. *IOP Conference Series: Materials Science and Engineering*, 2018, vol. 411 (1), p. 012012. DOI: 10.1088/1757-899X/411/1/012012.

31. Balanovsky A.E., Shtayger M.G., Kondrat'ev V.V., Nebogin S.A., Karlina A.I. Complex metallographic researches of 110G13L steel after heat treatment. *IOP Conference Series: Materials Science and Engineering*, 2018, vol. 411 (1), p. 012014. DOI: 10.1088/1757-899X/411/1/012014.

32. Kolosov A.D., Gozbenko V.E., Shtayger M.G., Kargapoltsev S.K., Balanovskiy A.E., Karlina A.I., Sivtsov A.V., Nebogin S.A. Comparative evaluation of austenite grain in high-strength rail steel during welding, thermal processing and plasma surface hardening. *IOP Conference Series: Materials Science and Engineering*, 2019, vol. 560, p. 012185. DOI: 10.1088/1757-899X/560/1/012185.

33. Karlina A.I., Balanovskiy A.E., Kondratiev V.V., Romanova V.V., Batukhtin A.G., Karlina Y.I. An investigation into the behavior of cathode and anode spots in a welding discharge. *Applied Sciences*, 2024, vol. 14 (21), p. 9774. DOI: 10.3390/app14219774.

34. Skeebe V.Yu., Ivancivsky V.V., Kutyshekin A.V., Parts K.A. Hybrid processing: the impact of mechanical and surface thermal treatment integration onto the machine parts quality. *IOP Conference Series: Materials Science and Engineering*, 2016, vol. 126 (1), p. 012016. DOI: 10.1088/1757-899x/126/1/012016.

35. Efremkov E.A., Martyushev N.V., Skeebe V.Yu., Grechneva M.V., Olisov A.V., Ens A.D. Research on the possibility of lowering the manufacturing accuracy of cycloid transmission wheels with intermediate rolling elements and a free cage. *Applied Sciences*, 2022, vol. 12 (1), vol. 5. DOI: 10.3390/app12010005.

36. Martyushev N.V., Skeebe V.Yu. The method of quantitative automatic metallographic analysis. *Journal of Physics: Conference Series*, 2017, vol. 803 (1), p. 012094. DOI: 10.1088/1742-6596/803/1/012094.

37. Skeebe V.Yu., Ivancivsky V.V. Reliability of quality forecast for hybrid metal-working machinery. *IOP Conference Series: Earth and Environmental Science*, 2018, vol. 194 (2), p. 022037. DOI: 10.1088/1755-1315/194/2/022037.

38. Zverev E.A., Skeebe V.Y., Skeebe P.Y., Khlebova I.V. Defining efficient modes range for plasma spraying coatings. *IOP Conference Series: Earth and Environmental Science*, 2017, 87(8), 082061, DOI: 10.1088/1755-1315/87/8/082061.

39. Skeebe V.Yu. Hybrid process equipment: improving the efficiency of the integrated metalworking machines initial designing. *Obrabotka metallov (tekhnologiya, oborudovanie, instrumenty) = Metal Working and Material Science*, 2019, vol. 21, no. 2, pp. 62–83. DOI: 10.17212/1994-6309-2019-21.2-62-83. (In Russian).



40. Borisov M.A., Lobanov D.V., Yanyushkin A.S., Skeebe V.Yu. Investigation of the process of automatic control of current polarity reversal in the conditions of hybrid technology of electrochemical processing of corrosion-resistant steels. *Obrabotka metallov (tekhnologiya, oborudovanie, instrumenty)* = *Metal Working and Material Science*, 2020, vol. 22, no. 1, pp. 6–15. DOI: 10.17212/1994-6309-2020-22.1-6-15. (In Russian).

41. Mamadaliev R.A., Bakhmatov P.V., Martyushev N.V., Skeebe V.Y., Karlina A.I. Influence of welding regimes on structure and properties of steel 12KH18N10T weld metal in different spatial positions. *Metallurgist*, 2022, vol. 65 (11–12), pp. 1255–1264. DOI: 10.1007/s11015-022-01271-9.

## Conflicts of Interest

The authors declare no conflict of interest.

© 2025 The Authors. Published by Novosibirsk State Technical University. This is an open access article under the CC BY license (<http://creativecommons.org/licenses/by/4.0>).